



C N R T
Matériaux
Basse-Normandie



CORNING

DOPAGE ET PROPRIETES THERMOELECTRIQUES DE L'OXYDE D'INDIUM $In_{2-x}M_xO_3$

*E. Guilmeau, D. Bérardan, D. Saurel, C. Simon, A. Maignan, and B. Raveau
CRISMAT Laboratory, Caen, France.*

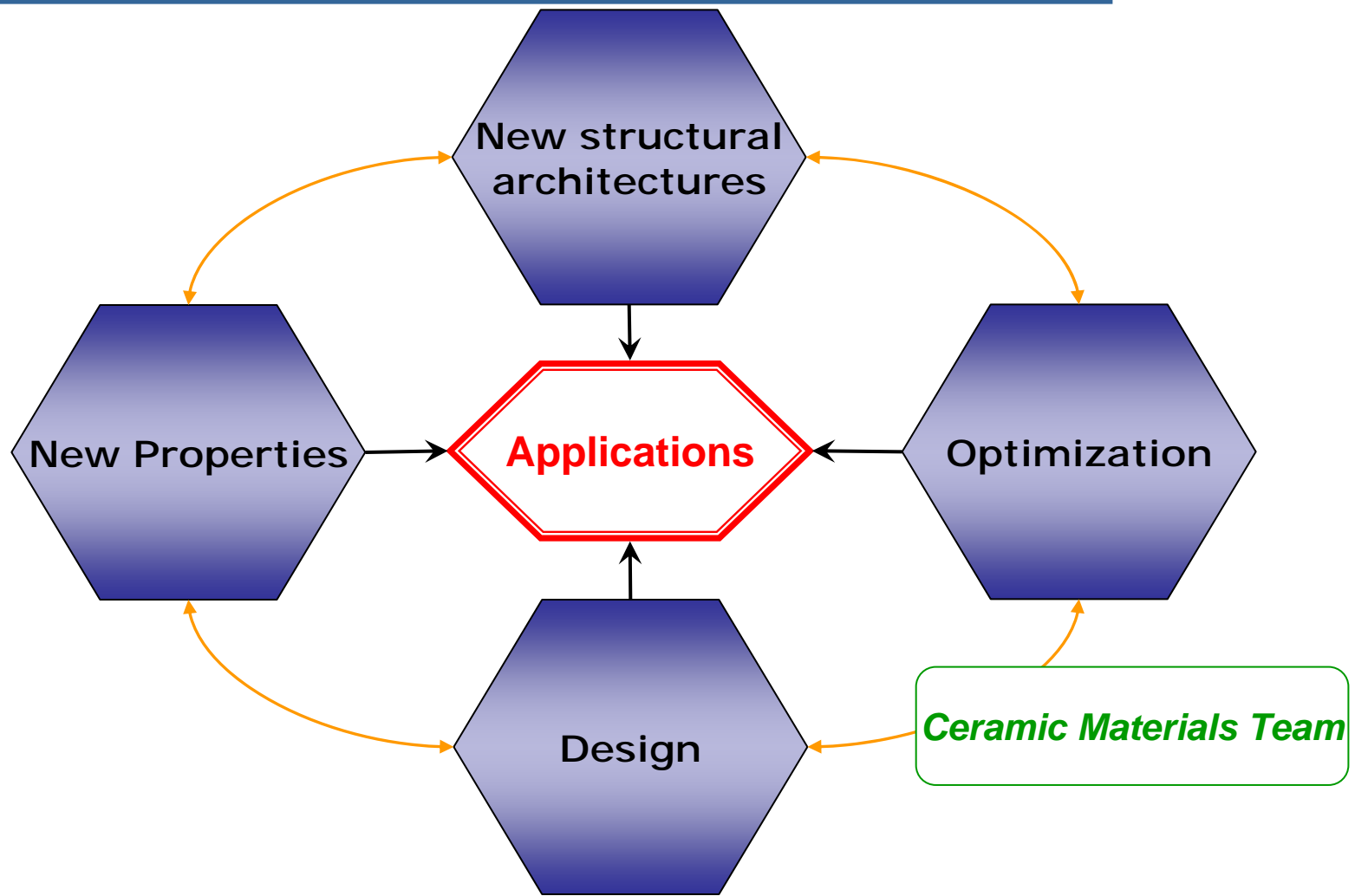
*F. Delorme
CORNING SAS, CETC, Avon, France*

Outline

- **Introduction:** Context of the Study
- $\text{In}_{2-x}\text{M}_x\text{O}_3$: *Dopant, Hall effect and TE properties*
- **Nanostructuration :** Prediction
- **Nanostructuration :** Preliminary results



CRISMAT Lab.



CRI SMAT & Thermoelectrics (1999-2009)

➤ A.C. Masset et al., *PR B* **62** (2000) 166

“Misfit layered cobaltite with an anisotropic giant magnetoresistance: $\text{Ca}_3\text{Co}_4\text{O}_9$ ”

➤ H. Leligny et al., *Acta Cryst. B* **56** (2000) 173

“A five-dimensional structural investigation of the misfit layer compound $[\text{Bi}_{0.87}\text{SrO}_2]_2[\text{CoO}_2]_{1.82}$ ”

➤ J. Hejtmanek et al., *PR B* **60** (1999) 14057

“Interplay between transport, magnetic, and ordering phenomena in $\text{Sm}_{1-x}\text{Ca}_x\text{MnO}_3$ ”

➤ M. Prevel et al., *Solid State Sci.* **9** (2007) 231

“Bulk textured $\text{Ca}_{2.5}\text{RE}_{0.5}\text{Co}_4\text{O}_9$ (RE: Pr, Nd, Eu, Dy and Yb) thermoelectric oxides by sinter-forging”

➤ S. Lemonnier et al., *J. Appl. Phys.* **104** (2008) 014505

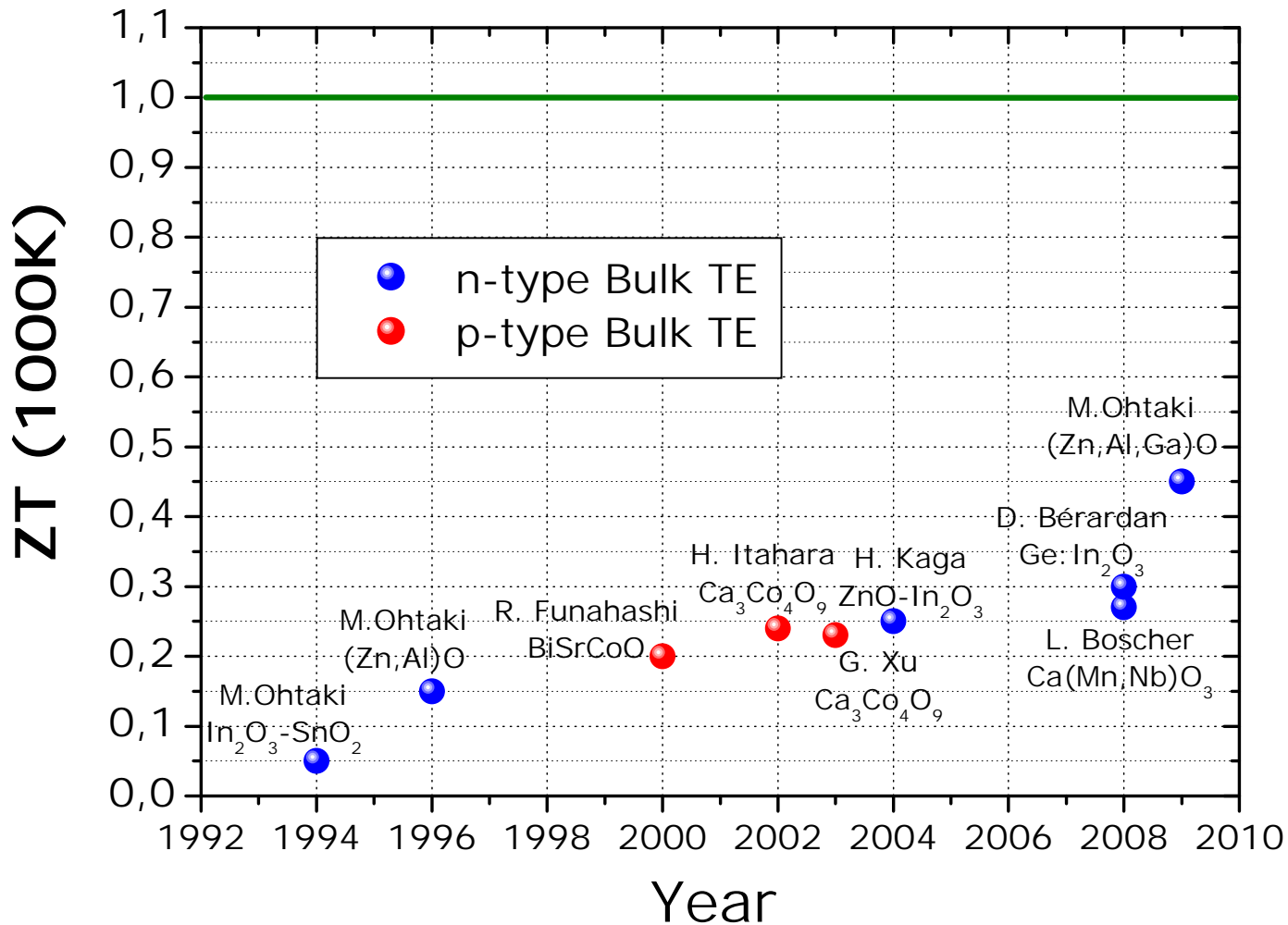
“Four-leg $\text{Ca}_{0.95}\text{Sm}_{0.05}\text{MnO}_3$ unileg thermoelectric device”

➤ D. Bérardan et al., *Solid State Comm.* **146** (2008) 97

“ $\text{In}_2\text{O}_3:\text{Ge}$, a promising n-type thermoelectric oxide composite”

Bulk Oxides

Bulk oxide Thermoelectrics



Ceramic Process

Nominal composition: $\text{In}_{2-x}\text{M}_x\text{O}_3$

Precursor Powders
Oxides or
carbonates

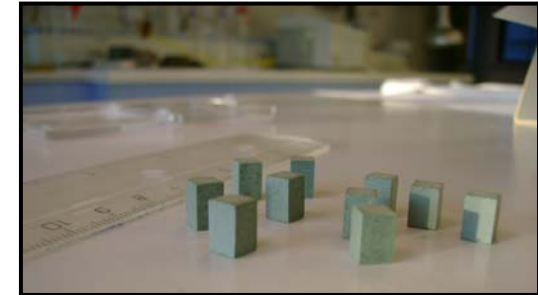


Ball-milling

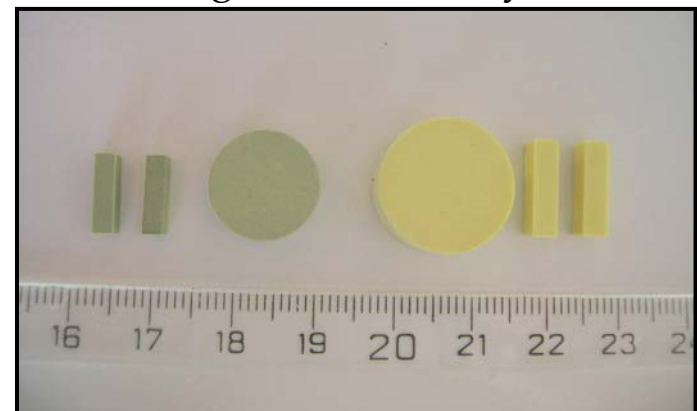


Bars/pellets shaping

Green density=60%



Shrinkage=15%, Density~90%



Sintering
 $1300^\circ\text{C}/48\text{h}$

Highly dense and pure samples

Facilities

Structure & Microstructure

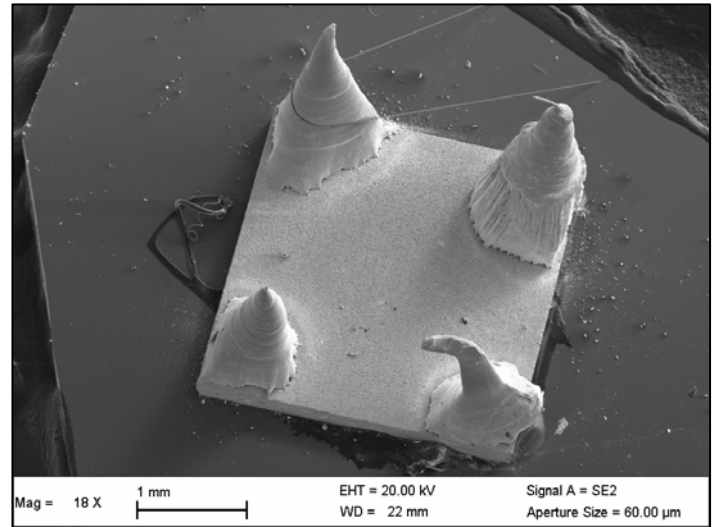
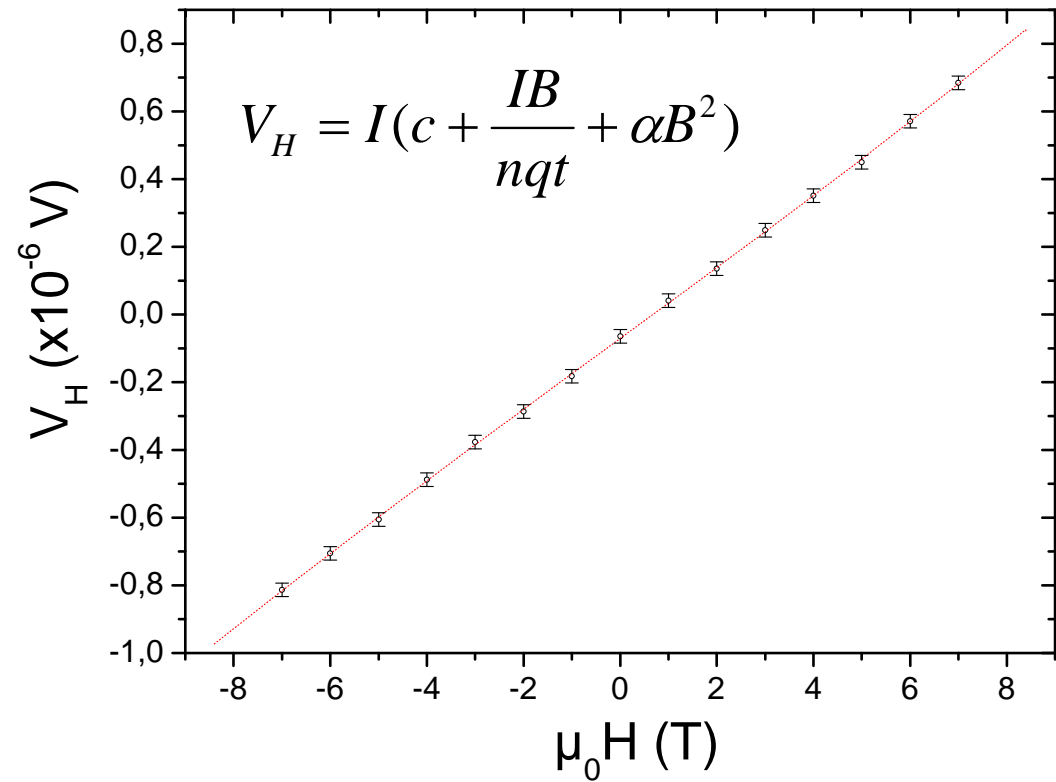
-X-ray & neutron diffraction, SEM, TEM, Grain size analyzer, dilatometer, TG/DTA, DSC...

HT Transport Properties

-ULVAC-RIKO, ZEM3 (Seebeck, resistivity → 800 °C)
-Netzsch, LFA 457 (thermal diffusivity → 1000 °C)
-Netzsch, DSC 404C (heat capacity → 1000 °C)
- PPMS (low T, ρ , λ , TEP, n)

Facilities

Hall Effect



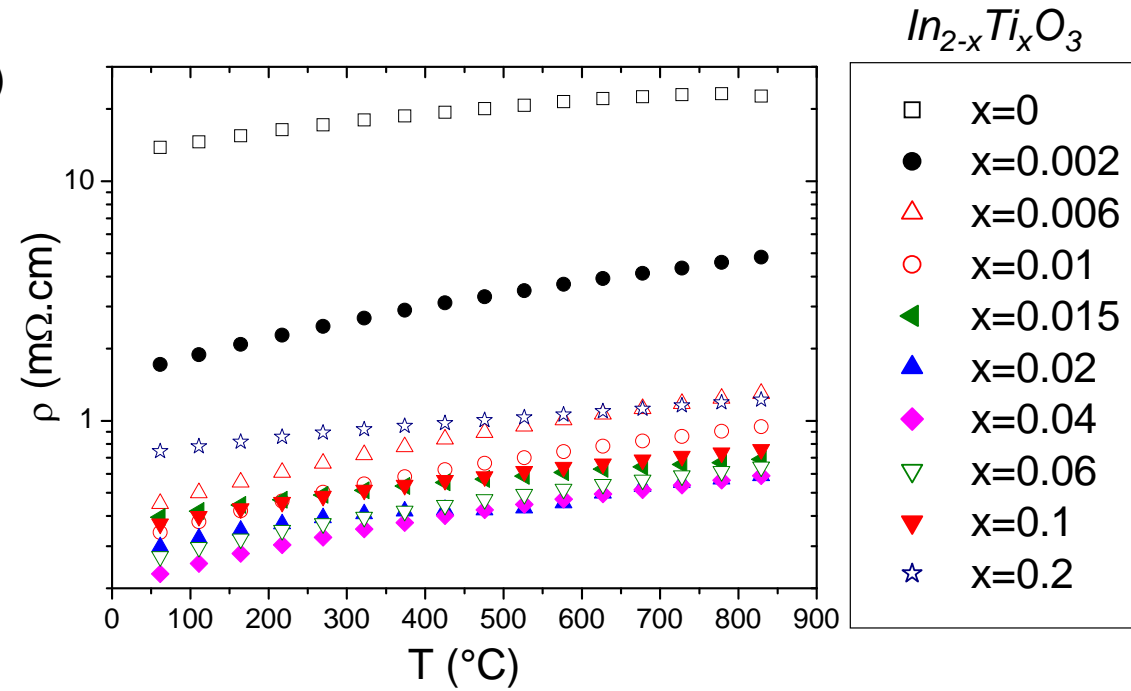
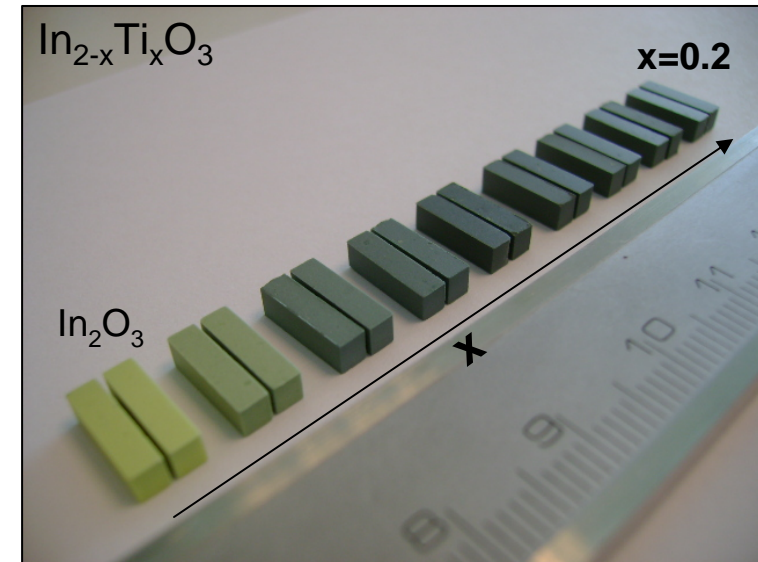
- Good ohmic contact
- Contact alignment, Thickness uniformity

Recent results: $\text{In}_{2-x}\text{M}^{4+}_x\text{O}_3$ and $\text{In}_{2-x}\text{M}^{5+}_x\text{O}_3$

« To clarify dopant and concentration effects is a key to understand and optimize the TE properties »*

$\text{In}_{2-x}\text{M}_x\text{O}_3$

- Tetravalent cations ($\text{M} \equiv \text{Sn}^{4+}, \text{Ti}^{4+}, \text{Zr}^{4+}$)
- Pentavalent cations ($\text{M} \equiv \text{Nb}^{5+}$ and Ta^{5+})

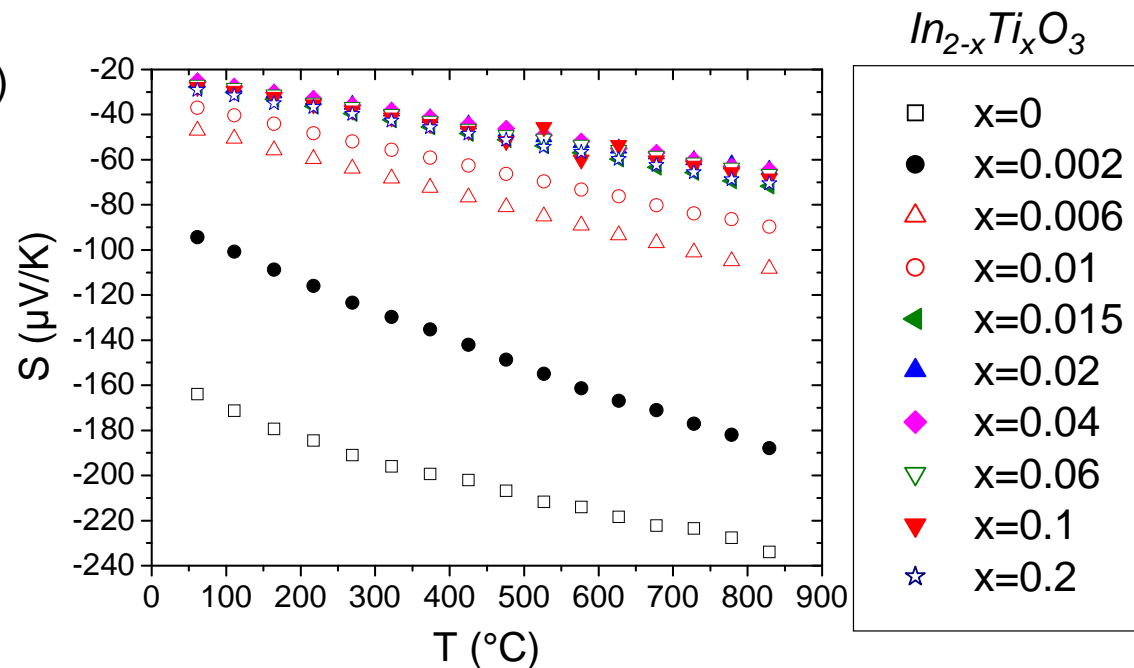
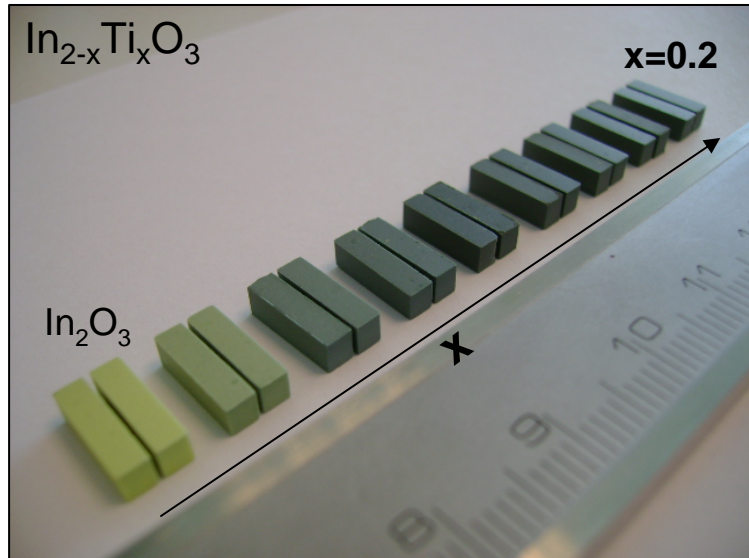


Recent results: $\text{In}_{2-x}\text{M}^{4+}_x\text{O}_3$ and $\text{In}_{2-x}\text{M}^{5+}_x\text{O}_3$

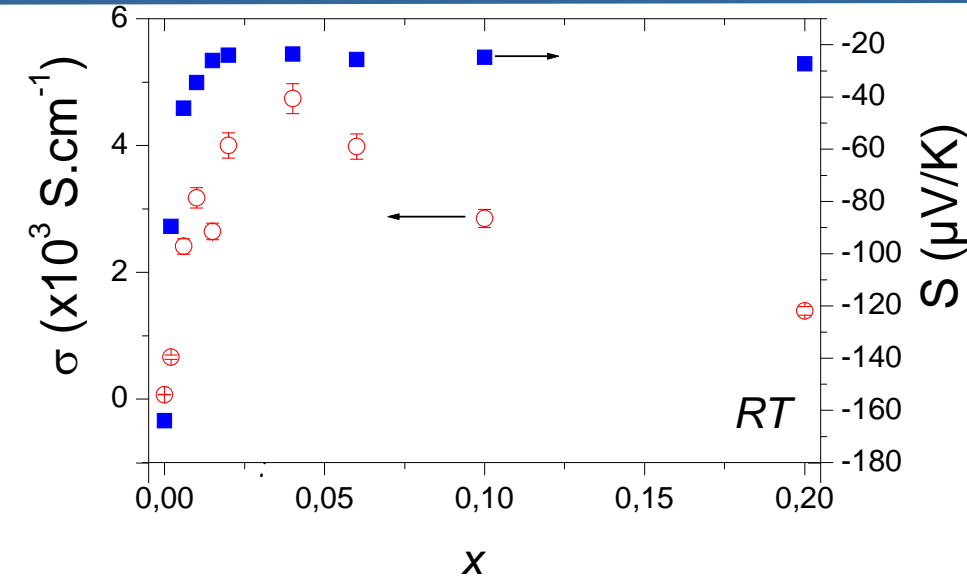
« To clarify dopant and concentration effects is a key to understand and optimize the TE properties »*

$\text{In}_{2-x}\text{M}_x\text{O}_3$

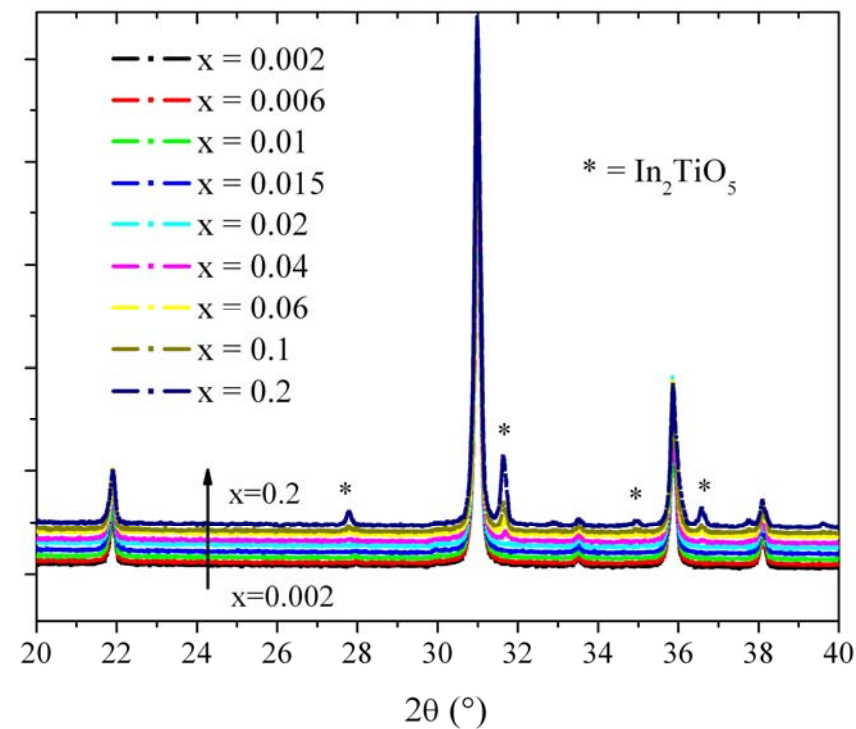
- Tetravalent cations ($\text{M} \equiv \text{Sn}^{4+}, \text{Ti}^{4+}, \text{Zr}^{4+}$)
- Pentavalent cations ($\text{M} \equiv \text{Nb}^{5+}$ and Ta^{5+})



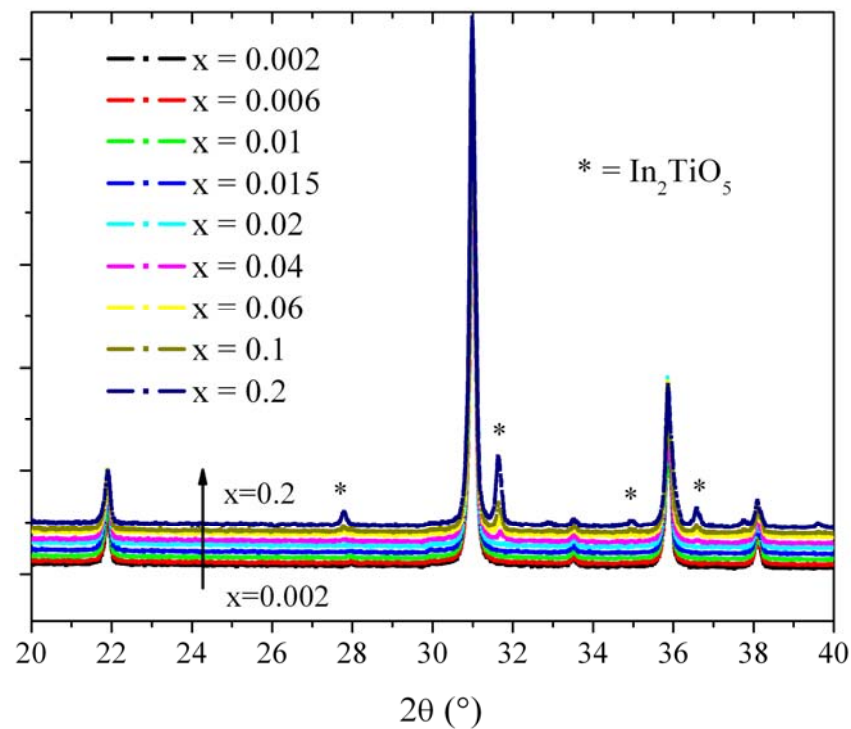
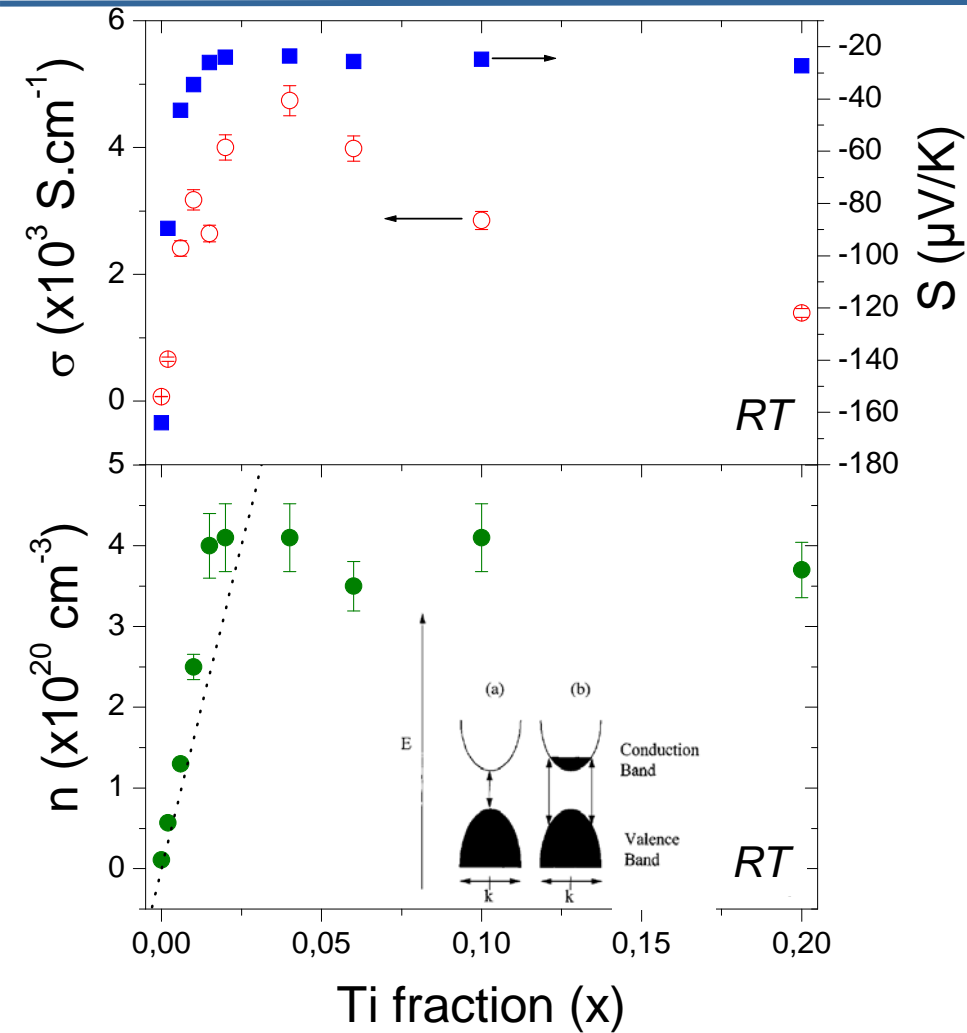
Recent results: $\text{In}_{2-x}\text{M}^{4+}_x\text{O}_3$ and $\text{In}_{2-x}\text{M}^{5+}_x\text{O}_3$



RT



Recent results: $\text{In}_{2-x}\text{M}^{4+}_x\text{O}_3$ and $\text{In}_{2-x}\text{M}^{5+}_x\text{O}_3$



- Ti^{4+} substitution generates 1 e- per dopant cation
- Additional donors



Recent results: $\text{In}_{2-x}\text{M}^{4+}_x\text{O}_3$ and $\text{In}_{2-x}\text{M}^{5+}_x\text{O}_3$

x ($\text{In}_{2-x}\text{M}_x\text{O}_3$)	S ($\mu\text{V.K}^{-1}$)					σ ($\times 10^3 \text{ S.cm}^{-1}$)				
	Sn^{4+}	Ti^{4+}	Zr^{4+}	Ta^{5+}	Nb^{5+}	Sn^{4+}	Ti^{4+}	Zr^{4+}	Ta^{5+}	Nb^{5+}
0.000	-163	-163	-163	-163	-163	0.08	0.08	0.08	0.08	0.08
0.002	-91	-90	-94	-75	-82	0.6	0.7	0.7	0.6	0.5
0.006	-53	-44	-55	-43	-43	1.4	2.4	1.8	1.9	1.7
0.01	-42	-35	-42	-42	-38	1.9	3.2	3.4	2.1	2.1
0.015	-35	-26	-28	-38	-36	1.8	2.6	3.6	1.9	2.3
0.02	-23	-24	-27	-41	-38	2.8	4.0	2.6	1.7	2.1
0.04	-22	-24	-26	-54	-39	4.5	4.7	2.6	0.9	1.8
0.06	-21	-26	-27	-52	-52	4.9	4.0	2.5	0.9	0.8
0.1	-20	-25	-28	-67	-64	4.5	2.8	1.5	0.4	0.7
0.2	-22	-27	-30	-60	-70	3.6	1.4	1.4	0.2	0.2

	n $\times 10^{20}$ (cm^{-3})					μ ($\text{cm}^2.\text{v}^{-1}.\text{s}^{-1}$)				
	Sn^{4+}	Ti^{4+}	Zr^{4+}	Ta^{5+}	Nb^{5+}	Sn^{4+}	Ti^{4+}	Zr^{4+}	Ta^{5+}	Nb^{5+}
0.000	0.11	0.11	0.11	0.11	0.11	41.8	41.8	41.8	41.8	41.8
0.002	0.58	0.57	0.51	1.36	1.16	58.2	72.6	85.9	27.2	26.1
0.006	1.8	1.26	1.45	3.2	2.03	50.1	119.5	76.1	36.1	52.2
0.01	2.56	2.6	2.77	4.5	3.54	47.5	76.3	77.3	29.1	37.6
0.015	3.4	3.98	2.55	2.78	4.32	33.3	41.5	40.2	43.7	33.6
0.02	6.77	4.1	2.93	2.9	2.87	25.6	36.2	56.3	37.7	44.8
0.04	6.9	4.15	2.88	1.58	3.36	40.9	71.4	56.2	35.3	32.6
0.06	9.43	3.56	1.93	1.54	1.92	32.4	69.9	73.6	39.02	28.1
0.1	10.8	4.09	2.61	1.1	1.66	25.9	43.5	7.6	22.1	27.1
0.2	8.55	3.68	1.66	1.4	1.54	26.0	23.6	9.6	10.9	9.0

- $|S|$ reaches minima for different x_ℓ
- σ reaches maxima for the similar x_ℓ
- n reaches maxima for the similar x_ℓ

Recent results: $\text{In}_{2-x}\text{M}^{4+}_x\text{O}_3$ and $\text{In}_{2-x}\text{M}^{5+}_x\text{O}_3$

x $(\text{In}_{2-x}\text{M}_x\text{O}_3)$	μ ($\text{cm}^2 \cdot \text{V}^{-1} \cdot \text{s}^{-1}$)				
	Sn^{4+}	Ti^{4+}	Zr^{4+}	Ta^{5+}	Nb^{5+}
0.000	41.8	41.8	41.8	41.8	41.8
0.002	58.2	72.6	85.9	27.2	26.1
0.006	50.1	119.5	76.1	36.1	52.2
0.01	47.5	76.3	77.3	29.1	37.6
0.015	33.3	41.5	40.2	43.7	33.6
0.02	25.6	36.2	56.3	37.7	44.8
0.04	40.9	71.4	56.2	35.3	32.6
0.06	32.4	69.9	73.6	39.02	28.1
0.1	25.9	43.5	7.6	22.1	27.1
0.2	26.0	23.6	9.6	10.9	9.0

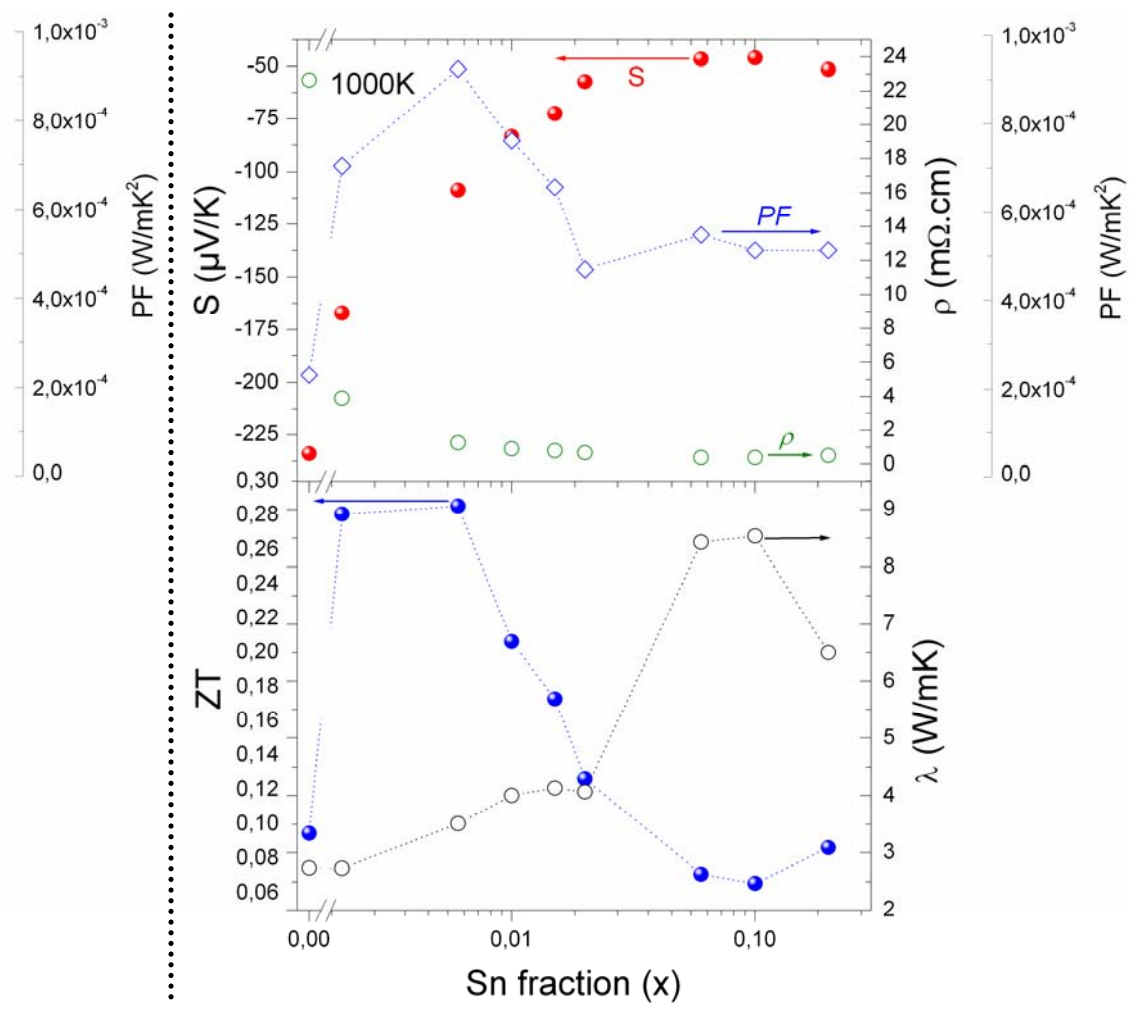
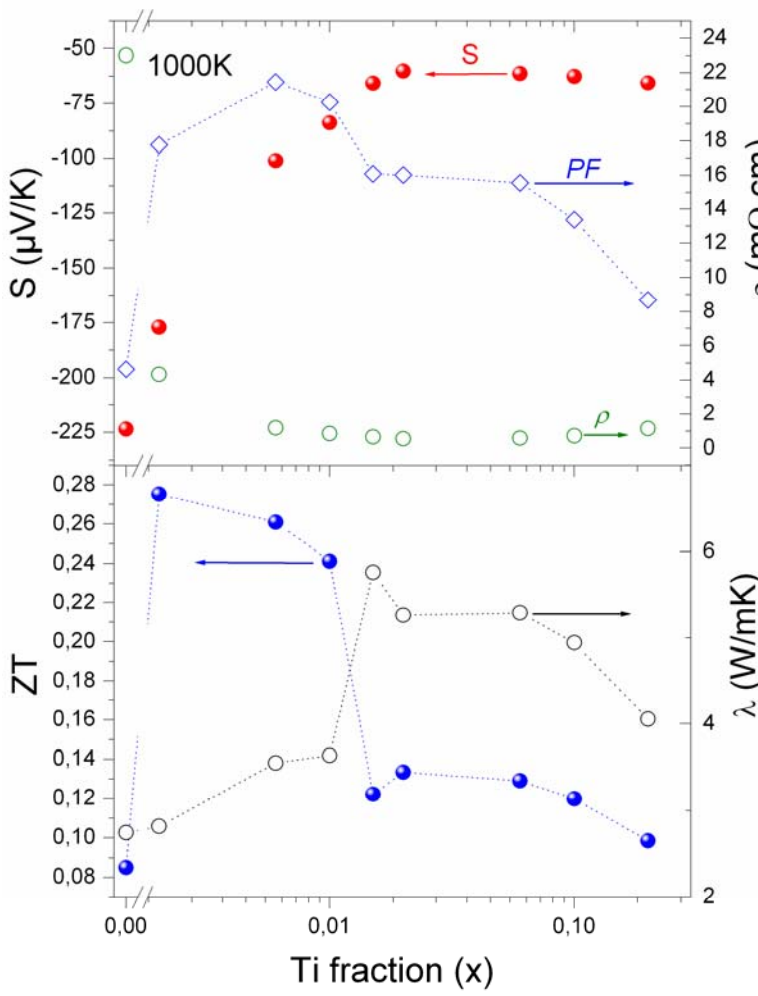
- $|S|$ reaches minima for different x_ℓ

- σ reaches maxima for the similar x_ℓ

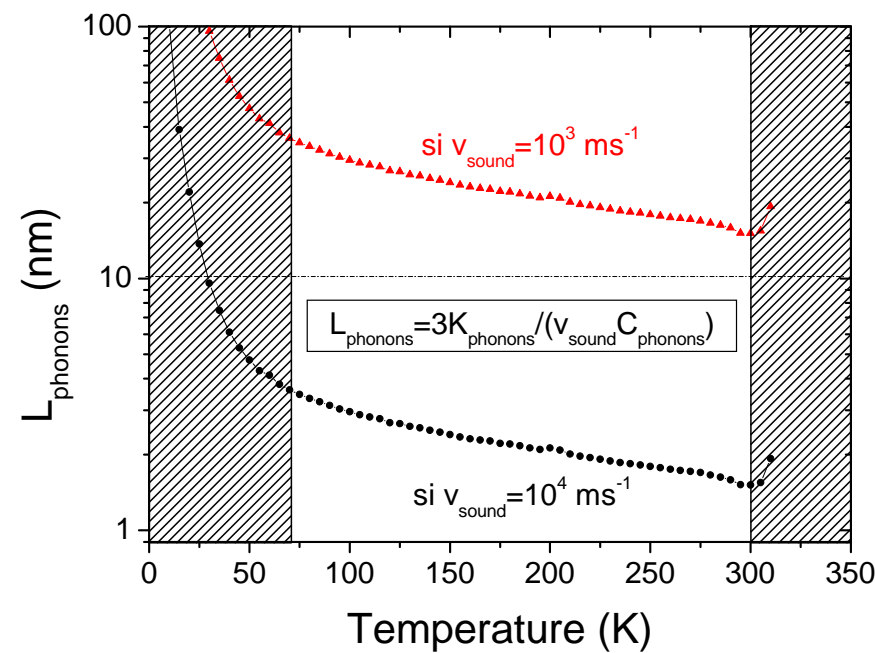
- n reaches maxima for the similar x_ℓ

- Higher mobilities for Sn, Ti and Zr at $x=0.006$
- Lower mobilities for Nb and Ta (e^-e^- scattering)

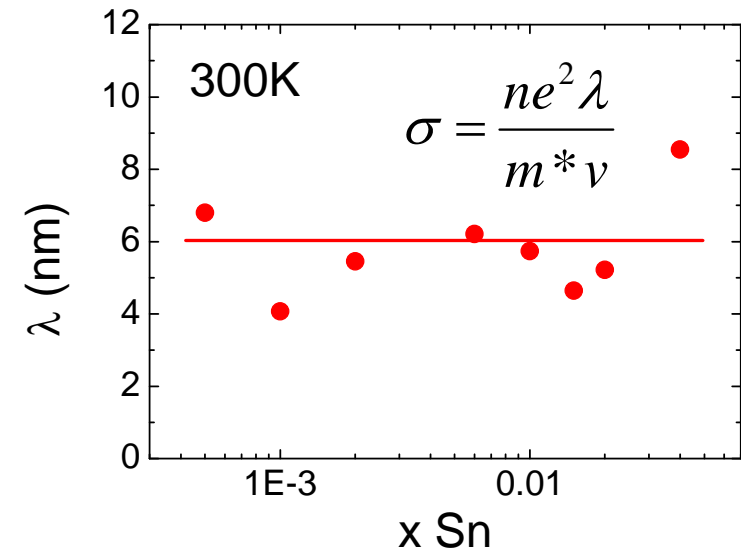
Recent results: $\text{In}_{2-x}\text{M}^{4+}_x\text{O}_3$ and $\text{In}_{2-x}\text{M}^{5+}_x\text{O}_3$



3D Nanostructuration: prediction



mfp ph ~ 2-10 nm

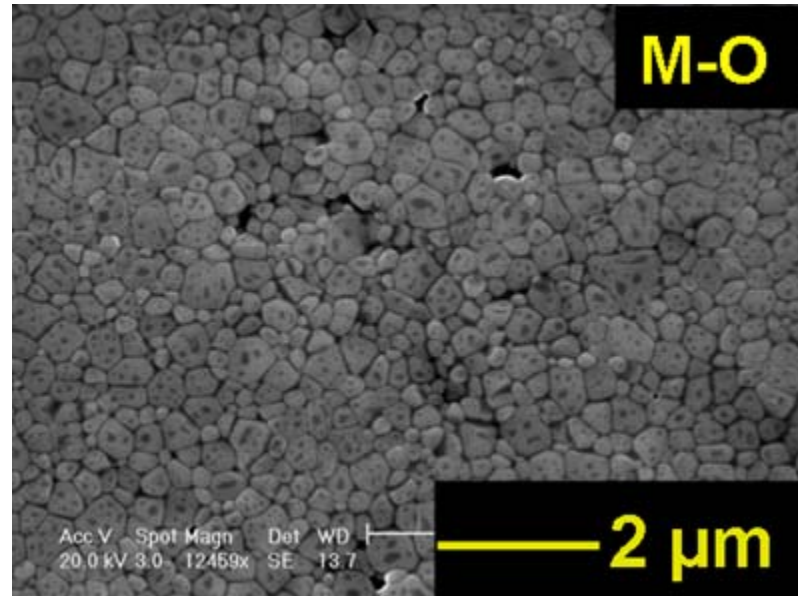
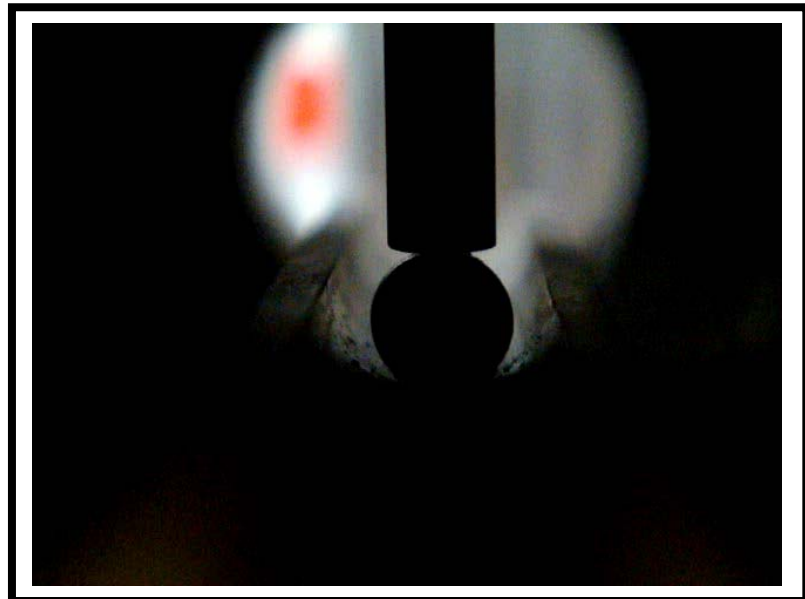


*Good agreement with J.R. Bellingham et al. J.P. Cond. Matter 2 (1990) 6207

mfp e⁻ ~ 6 nm

3D Nanostructuration: experimental

Nanoceramics processing



M-O

Thanks

for your attention!!!

Acc.V Spot Magn Det WD
20.0 kV 3.0 12459x SE 13.7

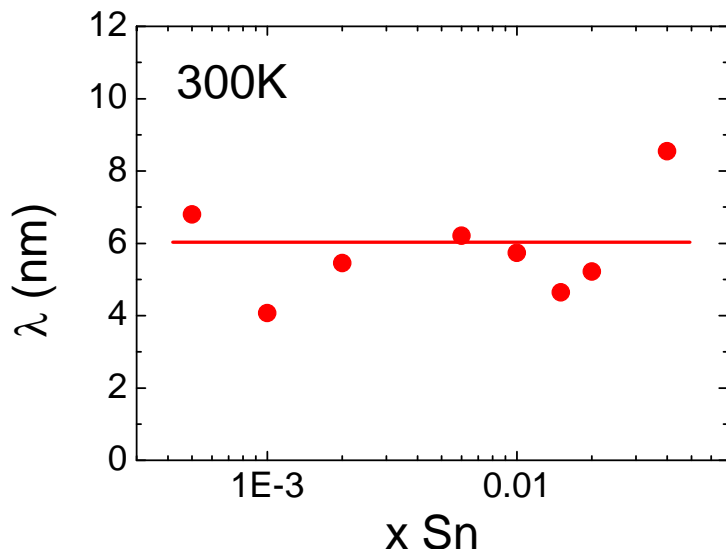
— 2 μm

Conductivité (modèle de Drude): $\sigma = \frac{ne^2\lambda}{m^*v}$

Vitesse des électrons : $v = \sqrt{v_{Fermi}^2 + v_{Thermique}^2}$

Vitesse thermique : $k_B T = \frac{1}{2} m^* v_{Thermique}^2$

Vitesse de Fermi (approximation parabolique): $v_{Fermi} = \frac{\hbar^2}{2m^*} (2\pi^2 n)^{2/3}$



Libre parcours moyen

- λ indépendant de x

- λ est faible (6 nm)

→ Nano-structuration fine possible pour optimiser le ZT